Unusual Stabilities of 6,6′-Bis(aminomethyl)-2,2′-bipyridyl Chelates of Transition-metal Ions and Crystal Structures of the Ligand and its Copper(II) and Nickel(II) Complexes†

Zheng Wang, Joseph Reibenspies, Ramunas J. Motekaitis and Arthur E. Martell*
Department of Chemistry, Texas A & M University, College Station, Texas 77 843–3255, USA

An improved four-step synthesis of the tetradentate compound 6,6′-bis(aminomethyl)-2,2′-bipyridyl (badp) has been developed and the crystal structure of its dihydrochloride monohydrate determined: space group $C2/c$, $a = 11.991(2)$, $b = 5.703(1)$, $c = 22.109(3)$ Å, $\beta = 97.17(1)°$ and $Z = 4$. The complexes of copper(II) and nickel(II) with badp have also been synthesized and structurally characterized. The metal ion in $[Cu(badp)(H_2O)]Br_2$ is five-co-ordinated and the complex crystallizes in the monoclinic $P2_1/c$ space group with $a = 11.508(3)$, $b = 9.584(3)$, $c = 14.362(3)$ Å, $\beta = 107.93(2)°$ and $Z = 4$. The complex $[Ni(badp)(H_2O)Br]Br$ contains six-co-ordinated Ni^{II} and crystallizes in the monoclinic $P2_1/c$ space group with $a = 11.387(3)$, $b = 9.417(2)$, $c = 14.317(5)$ Å, $\beta = 106.21(2)°$ and $Z = 4$. The stepwise stability constants of the 1:1 ligand to metal complexes of badp with divalent transition-metal ions have been determined in KCl as supporting electrolyte (0.100 mol dm^{-3}) at 25.0 °C: log $K_{ML} = [ML]/[M][L]$ for the Fe^{II}, Co^{II}, Ni^{II}, Cu^{II} and Zn^{II} complexes is 8.94, 10.16, 11.87, 15.05 and 10.02 respectively. Iron(II) and cobalt(II) also formed 2:1 complexes with badp. The unusually low stabilities of the transition-metal complexes are considered due to the low basicity of the ligand and to the unfavourable spacing of its donor groups as indicated by the structures of the complexes of Ni^{II} and Cu^{II}.

In recent years interest in the design and synthesis of a large number of photoactive cryptands[1,2] and polyfunctionalized macrocyclic ligands[3–5] has resulted in the study of the co-ordination chemistry of polydentate bipyridyl-containing chelating ligands.[6,7] This paper describes the synthesis of a tetradentate ligand 6,6′-bis(aminomethyl)-2,2′-bipyridyl (badp) and the determination of the crystal structure of its dihydrochloride salt. This polyamine was prepared as an intermediate for the synthesis of bipyridyl-containing dinucleating macrocyclic ligands by the 2 + 2 condensation of dialdehydes and polyamines to form Schiff bases. However it is interesting as a tetraaza ligand in its own right, especially in view of its unusual properties, based on the stabilities of the complexes of Cu^{II} and Ni^{II} in solution, their comparison with complexes of analogous ligands, and rationalization of the stabilities on the basis of relative basicities and the crystal structures of the complexes.

In view of the very limited work reported on complexes of polydentate bipyridyls[6,8] the preparation and characterization of complexes formed by reaction of this compound with a series of divalent transition-metal ions are also reported. The protonation constants of the trihydrobromide salt of badp, as well as the binding constants with divalent metal ions Fe^{II}, Co^{II}, Ni^{II}, Cu^{II} and Zn^{II}, are determined potentiometrically. Furthermore, potentiometric studies of the formation of 2:1 ligand:metal ion complexes with Fe^{II} and Co^{II} are also reported. A five-co-ordinated environment for the copper(II) complex and a six-co-ordinated arrangement for the nickel(II) complex are found in the solid state as demonstrated by the determination of the crystal structures of $[Cu(badp)(H_2O)]Br_2$ and $[Ni(badp)(H_2O)Br]Br$.

Results and Discussion

Synthesis.—The synthetic pathway to the trihydrobromide salt of the tetradentate badp and eventually to its complexes with divalent transition-metal ions is illustrated in Scheme 1. The synthesis of the tetrahydrochloride under different experimental conditions (concentrated hydrochloric acid) was reported by Alpha *et al.*[1] To our knowledge, this is first report of the preparation and the crystal structure analysis of the dihydrochloride badp·2HCl·H_2O and of its divalent metal-ion complexes $[Ni(badp)(H_2O)Br]Br$ and $[Cu(badp)(H_2O)]Br_2$.

The first two synthetic steps in Scheme 1 under different experimental conditions were reported previously.[6] The advantages of the present reaction conditions are greater quantity of material and higher overall yield, 58% (*ca.* 45% reported previously[6]). In the first step the reaction mixture was made alkaline (pH > 11) in order to convert the excess of Br_2 into other forms soluble in water and to remove them completely in the extraction. The reaction is: $3Br_2 + 6OH^- \longrightarrow 5Br^- + BrO_3^- + 3H_2O$. The excess of Br_2 is undesirable because it reacts with the desired product in the purification process to form the dibromo-substituted by-product 5,6-dibromo-2-methylpyridine. The improvement in this synthetic step reduces the by-product dramatically. Furthermore, in the second step, a more efficient catalyst (10% wet Pd/C) was chosen and the reaction time was expanded to 7 d. These modifications increased the yield sufficiently so that the desired product 6,6′-dimethyl-2,2′-bipyridine can be crystallized from the crude oil. In the third synthetic step the conditions described previously[7] produce mostly the monobromide product. Therefore, the amount of *N*-bromosuccinimide was adjusted to 5% excess and the reaction time was expanded to 6 h, and chloroform was used to remove the excess of succinimide from the crude product in the recrystallization process. The experimental conditions described in this research achieve the overall yield of 23% for the four-step synthesis based on the starting amine.

† *Supplementary data available:* see Instructions for Authors, *J. Chem. Soc., Dalton Trans.*, 1995, Issue 1, pp. xxv–xxx.
Non-Si unit employed: mmHg ≈ 133 Pa.

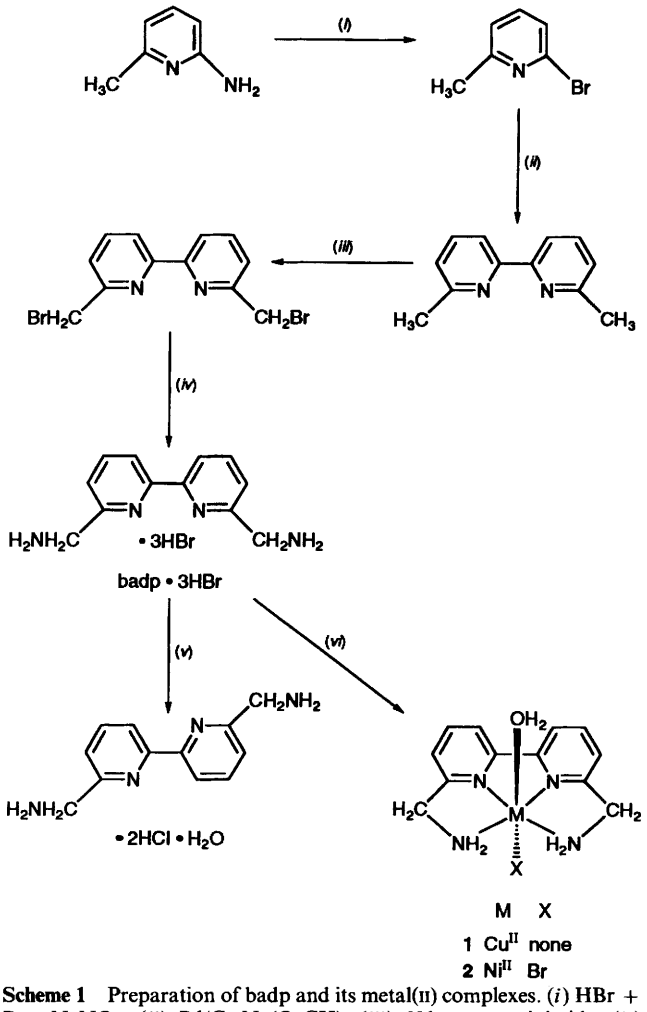

Scheme 1 Preparation of badp and its metal(II) complexes. (*i*) HBr + Br_2, $NaNO_2$; (*ii*) Pd/C, $Na(O_2CH)$; (*iii*) *N*-bromosuccinimide; (*iv*) hexamethylenetetramine, HBr + EtOH; (*v*) NaCl, NaOH; (*vi*) M^{II}

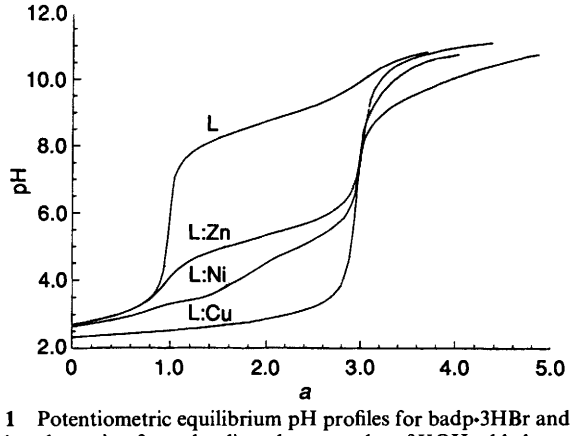

Fig. 1 Potentiometric equilibrium pH profiles for badp•3HBr and for a 1:1 molar ratio of metal to ligand. *a* = moles of KOH added per mol of badp present. Total concentrations: $c_L = 1.010 \times 10^{-3}$, $c_{Zn} = 1.005 \times 10^{-3}$, $c_{Ni} = 1.002 \times 10^{-3}$, $c_{Cu} = 1.008 \times 10^{-3}$ mol dm^{-3}. There are approximately 10 equilibrium points per *a* value. 25.0 °C, $I = 0.100$ mol dm^{-3} (KCl)

Protonation Constants of badp•3HBr•H_2O.—The potentiometric equilibrium pH (where pH = $-\log [H^+]$) profile of badp•3HBr•H_2O in the absence of metal ions is shown as the top curve in Fig. 1, and the corresponding protonation constants computed by BEST[9] are given in Table 1, along with the literature values for 2,6-bis(aminomethyl)pyridine (bap),[10] 2-(aminomethyl)pyridine (ap),[11] triethylenetetramine (trien),[11] and *N*,*N*′-bis(2-pyridylmethyl)ethylenediamine (bpmen),[12]

Table 1 Logarithms of successive protonation constants of badp and for related compounds

	badp[a]	bap[b]	ap[c]	bpmen[d]	trien[e]
$\log K_{HL}$	9.11 ± 0.02	9.53	8.61	8.23	9.74
$\log K_{H_2L}$	8.39 ± 0.02	9.15	2.0	5.45	9.07
$\log K_{H_3L}$	1.2 ± 0.2			1.81	6.59
$\log K_{H_4L}$				1.62	3.27

[a] This work: $\sigma_{fit} = 0.006$, average of three titrations; 25.0 °C, $I = 0.100$ mol dm^{-3} (KCl). [b] 20.0 °C, $I = 1.0$ mol dm^{-3}.[10c] 25.0 °C, $I = 0.100$ mol dm^{-3}. [d] Ref. 12. [e] Ref. 11.

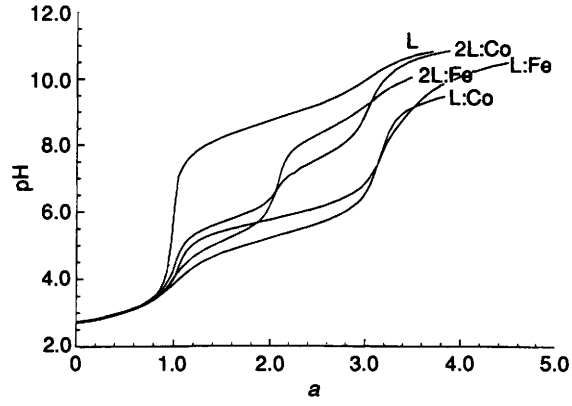

Fig. 2 Potentiometric equilibrium pH profiles of 1.010×10^{-3} mol dm^{-3} ligand badp•3HBr in the absence of metal ion and in the presence of 1:1 and 2:1 molar ratios of ligand to Co^{II} and Fe^{II} as indicated. *a* = Moles of base added per mol of ligand present; 25.0 °C, $I = 0.100$ mol dm^{-3}, adjusted with KCl

which may be considered related to badp because it has similar functional groups. The potentiometric titration further confirmed the formula of the hydrobromide form as badp•3HBr•H_2O, which agrees with the results found by elemental analysis (Experimental section). The internal consistency is evidenced by the overall $\sigma_{fit} = 0.006$ in each of the three parallel titration experiments, and the standard deviations of these titrations.

The potentiometric titration curve for badp shown in Fig. 1 has a flat, low-pH buffer region up to $a = 1.0$ (a = moles of base per mol of ligand) which indicates strong acid character of the proton bound to one of the bipyridyl nitrogen atoms (log $K_3^H = [H_3L^{3+}]/[H_2L^{2+}][H^+] = 1.2$). This is followed by a steep inflection and another flat buffer region from $a = 1$ to $a = 3$ indicating two overlapping basic sites, the aminomethyl groups. Considering that badp can be prepared as a tetrahydrochloride only under very acidic conditions,[1] the fourth protonation constant corresponding to protonation of the other bipyridyl nitrogen atom must be too low to be measured by potentiometry. In this laboratory, only the trihydrochloride could be isolated even from strong HCl solution. The measured protonation constants of badp are comparable to those of the corresponding groups of bpmen,[12] trien[11] and ap[11] shown in Table 1.

Stability Constants.—The 1:1 and 2:1 L:M complex formation constants of badp with divalent metal ions were determined in 1:1 and 2:1 solutions from the potentiometric equilibrium pH profiles shown in Figs. 1 and 2. The stability constants listed in Table 2 show that the order of stability for chelates of the divalent metal ions is $Cu \gg Ni^{II} > Co^{II} > Zn^{II} > Fe^{II}$. A similar order was found for the somewhat related ligand bpmen[12] shown in Table 2. It is noted that there are few examples of stability constants of iron(II) complexes of polydentate bipyridyl ligands with various amino donors in the

Table 2 Logarithms of formation constants of metal chelates of badp [I = 0.100 mol dm^{-3} (KCl); 25.0 °C; under argon]

Equilibrium quotient	M = Fe^{II}	Co^{II}	Ni^{II}	Cu^{II} [a]	Zn^{II}
[ML]/[M][L] [b]	8.94	10.16	11.87	15.05	10.02
[M(HL)]/[ML][H] [b]	5.08	4.85	4.93	3.29	4.86
$[ML_2]/[ML][L]$ [b]	3.54	5.66	*c*	*c*	*c*
[M(OH)L][H]/[ML] [b,d]	−9.38	−8.68	−10.72	−6.01	−9.46
[ML']/[M][L'] [e]	*c*	12.8 [e]	14.4 [e]	16.3 [e]	11.5 [e]
[ML'']/[M][L''] [f]	7.76	10.9	13.8	20.1	12.0

[a] Values from tren [tris(2-aminoethyl)amine] competition titration measurement. [b] Estimated errors are 0.03% or less. [c] Not measured. [d] Proton dissociation from $ML(OH_2)$ to form M(OH)L. [e] L' = bpmen, ref. 12. [f] L'' = trien, ref. 11.

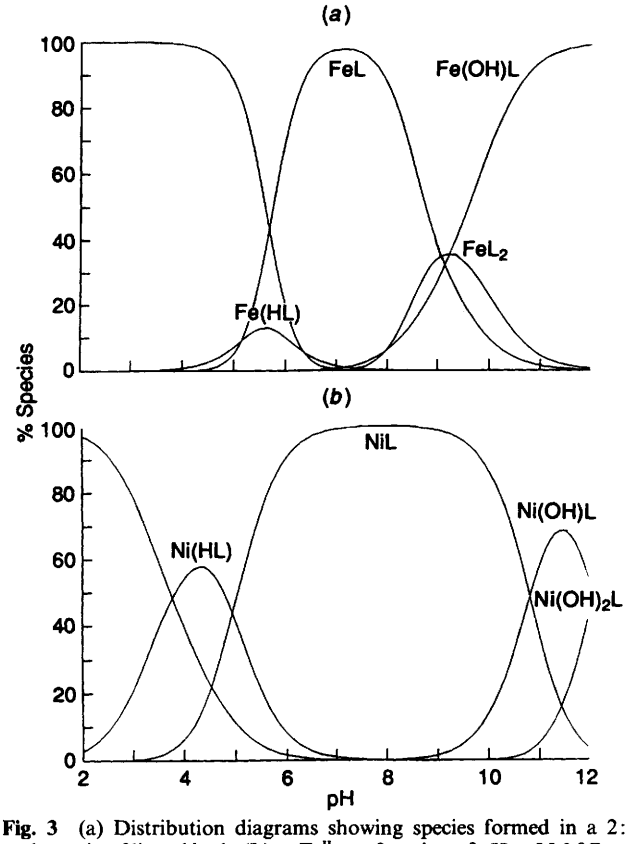

Fig. 3 (a) Distribution diagrams showing species formed in a 2:1 molar ratio of ligand badp (L) to Fe^{II} as a function of pH at 25.0 °C and 0.100 mol dm^{-3} ionic strength (KCl). $c_L = 2\ c_{Fe} = 1.01 \times 10^{-3}$ mol dm^{-3} (*b*) Distributions of species as a function of pH for the 1:1 Ni–badp system at 25.0 °C and 0.100 mol dm^{-3} ionic strength (KCl). Curves show percent of complex formed relative to total concentrations of badp or Ni^{II} present. They apply only to the rapid or moderately rapid nickel complex equilibria. The very slow reaction to form the 2:1 NiL_2 complex is not considered

literature, probably because the complexes are susceptible to oxidation by dioxygen in air and therefore require special precautions.

The pH profiles for the 2:1 solutions with Fe^{II} and Co^{II} (Fig. 2) show an inflection at a = 2.0 indicative of the formation of the 1:1 metal complex (1.5 a for the 1:1 complex and 0.5 a for the remaining free badp). The second inflection at a = 3 indicates the formation of the 2:1 complex. The stability constant of the $Co^{II}L_2$ complex is also larger than that of $Fe^{II}L_2$ (Table 2). Besides the 1:1 and 2:1 complexes, protonated complexes M(HL) and hydroxo complexes M(OH)L are also formed, depending on the pH of the solution. There was qualitative evidence for the very slow formation of a 2:1 nickel(II) complex, but the reaction was so slow (about 5 h per experimental point) that an experimental value of the equilibrium constant was not measured. There was no potentiometric evidence for the formation of 2:1 constants of

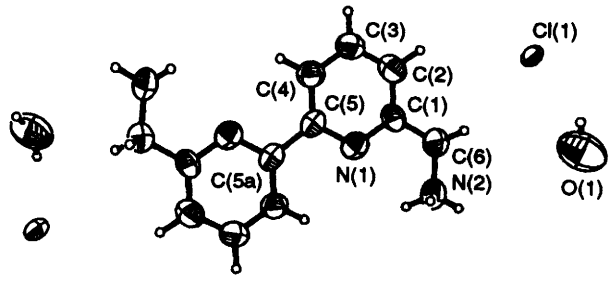

Fig. 4 Thermal ellipsoid plot (50%) and atom numbering scheme for badp·2HCl·H_2O

Cu^{II} and Zn^{II}. The UV/VIS absorption curve (Fig. 7) of the 1:1 copper(II) complex was not affected by an excess of badp, indicating that Cu^{II} does not form 2:1 complexes in dilute solution.

Typical species distribution curves of the system Fe^{II}–badp are shown in Fig. 3(*a*). It is seen that the maximum concentration of monoprotonated complex Fe(HL) (14%) is reached at pH 5.7, followed by the ligand–metal complex FeL attaining its maximum concentration (96%) at pH 7.4. The conversion of the 1:1 into the 2:1 complex occurs about pH 8, and the FeL_2 species reached 35% at pH 9.2. Above that pH the hydroxo complex Fe(OH)L becomes the dominant form. The distribution curves of the Ni^{II}–badp system shown in Fig. 3(*b*) indicate that the metal ion is more than 95% complexed as the ML form from pH 6.6 to 9.1, and that it is the predominant species between pH 4.9 and 10.7. Within the large pH range available, pH 7.1 was chosen for growth of the single crystal of the 1:1 nickel(II) complex.

Molecular Structure of badp·2HCl·H_2O.—The structure of badp was determined by crystallographic analysis of its dihydrochloride monohydrate salt, in which two amino nitrogen atoms and two aromatic nitrogen atoms of bipyridyl are located at complementary positions through an inversion centre. Thus, the molecular structure shown in Fig. 4 has C_{2h} symmetry. Atomic coordinates, bond lengths and angles are given in Tables 3 and 4. A summary of crystallographic results is given in Table 5.

It is very likely that the repulsion of the positive charges in the protonated amines forces the compound to adopt this geometry. The configuration is significant since the compound adopts C_{2v} symmetry with the disappearance of the inversion centre when it binds to metal ions to form complexes, see below. The chloride anions function not only for charge balance but also for the linkage of the protonated ammonium groups by coulombic attraction to form a chain-like structure. Water molecules fill in the spaces between the badp molecules without the formation of hydrogen bonds.

Structures of [Cu(badp)(H_2O)]Br_2 **1** *and* [Ni(badp)(H_2O)-Br]Br **2**.—The ORTEP[13] plots of complexes **1** and **2** with labelling schemes are shown in Fig. 5. Tables of atomic coordinates and selected bond lengths and angles for both

molecules are given in Tables 6 and 7, respectively. The crystallographic results are summarized in Table 5.

Compound **1** crystallizes in the space group $P2_1/c$ with the complex cation, one water molecule and two bromide ions in the unit cell. The complex exhibits a five-co-ordinated motif in a distorted square pyramid around the copper centre. The copper(II) ion is co-ordinated to two primary amino nitrogen atoms [N(3), N(4)] and two aromatic nitrogen atoms [N(1), N(2)] of the badp ligand and an oxygen atom of a water molecule occupying the axial position.

The configuration of this compound is comparable to that adopted in [Cu(trien)(SCN)]NCS,[14] in which the complex also has a distorted square-pyramidal structure, with an S atom in the apical position. The copper atom is 0.37 Å above the plane so that the mean value of the four N–Cu–S bond angles is 100.7°, while the four nitrogen atoms are alternately above and below the plane that forms the base of the square pyramid. This distortion is common to many aliphatic polyamine copper complexes such as Cu(en) and Cu(trien). In [Cu(trien)-(SCN)]NCS the intrachelate N–Cu–N bond angles are 84.3, 84.7, and 84.6°, but that of the open side of the trien group is 98.9°.

There are considerable differences in the structures of [Cu(trien)(SCN)]NCS and [Cu(badp)(H_2O)]Br_2. The distortion of the co-ordination environment in complex **1** is best illustrated by the deviation of the equatorial N–Cu–N bond angles from 90°. For example, the angle between the metal ion

Table 3 Atomic coordinates ($\times 10^4$) for badp·2HCl·H_2O

Atom	*x*	*y*	*z*
Cl(1)	3471(1)	1163(2)	6777(1)
O(1)	5000	7028(13)	7500
N(1)	624(4)	8556(7)	5679(2)
N(2)	1190(4)	8194(8)	6875(2)
C(1)	1282(5)	6677(9)	5848(3)
C(2)	1678(5)	5193(11)	5430(3)
C(3)	1405(5)	5641(10)	4824(3)
C(4)	755(4)	7569(10)	4650(3)
C(5)	366(4)	8977(9)	5077(2)
C(6)	1498(5)	6211(10)	6514(3)

Table 4 Bond lengths (Å) and angles (°) for badp·2HCl·H_2O

N(1)–C(5)	1.349(6)	N(1)–C(1)	1.355(6)
N(2)–C(6)	1.459(7)	C(1)–C(2)	1.380(8)
C(1)–C(6)	1.487(8)	C(2)–C(3)	1.363(8)
C(3)–C(4)	1.374(8)	C(4)–C(5)	1.365(7)
C(5)–C(5a)	1.474(10)		
C(5)–N(1)–C(1)	117.9(5)	N(1)–C(1)–C(2)	122.5(5)
N(1)–C(1)–C(6)	116.0(5)	C(2)–C(1)–C(6)	121.4(5)
C(3)–C(2)–C(1)	118.8(6)	C(2)–C(3)–C(4)	118.9(5)
C(5)–C(4)–C(3)	120.5(6)	N(1)–C(5)–C(4)	121.4(5)
N(1)–C(5)–C(5a)	115.2(5)	C(4)–C(5)–C(5a)	123.4(6)
N(2)–C(6)–C(1)	112.3(5)		

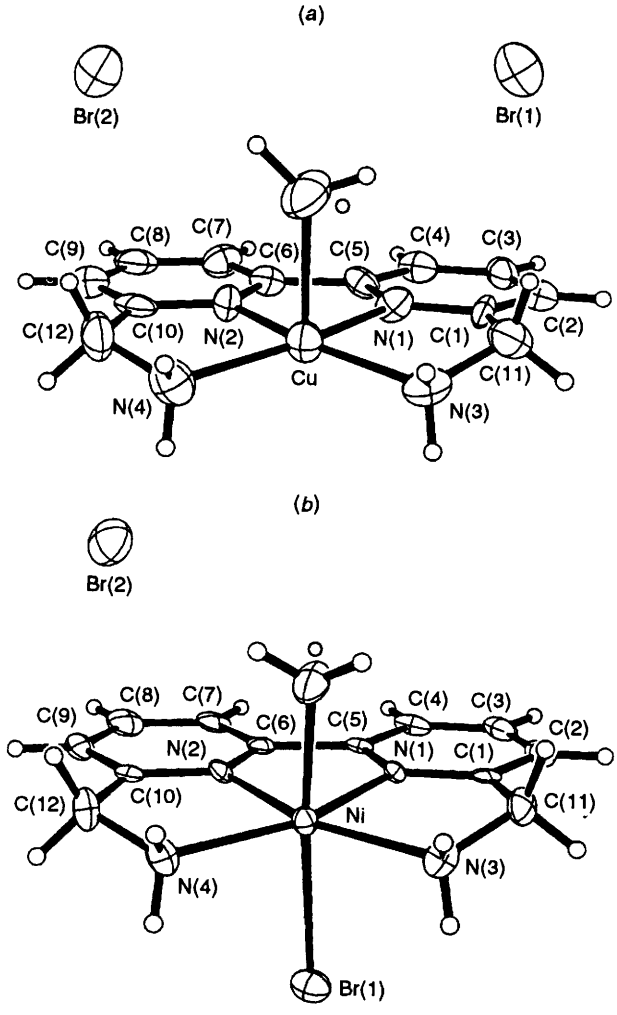

Fig. 5 Thermal ellipsoid plots (50%) and atomic numbering schemes for complexes **1**(*a*) and **2**(*b*)

Table 5 Summary of crystallographic results for compounds badp·2HCl·H_2O, **1** and **2**

	badp·2HCl·H_2O	**1**	**2**
Empirical formula	$C_{12}H_{18}Cl_2N_4O$	$C_{12}H_{16}Br_2CuN_4O$	$C_{12}H_{16}Br_2N_4NiO$
M	305.2	455.6	450.78
Space group	*C*2/*c*	$P2_1/c$	$P2_1/c$
a/Å	11.991(2)	11.508(3)	11.387(3)
b/Å	5.703(1)	9.584(3)	9.417(2)
c/Å	22.109(3)	14.362(3)	14.317(5)
β/°	97.17(1)	107.93(2)	106.21(2)
U/Å^3	155.1(4)	1507.1(7)	1474(7)
D_c/g cm^{-3}	1.36	1.99	2.03
μ/mm^{-1}	0.430	6.78	8.26
F(000)	700	892	888
Radiation (λ/Å)	Mo (0.710 73)	Mo (0.710 73)	Cu (1.541 78)
$R(F)$ [$I > 2\sigma(I)$]	0.0600	0.0677	0.0458
$R'(F^2)$ [$I > 2\sigma(I)$]	0.1639	0.2916	0.1416
$S(F^2)$	1.033	1.110	1.098

Details in common: monoclinic, $Z = 4$; 293 K; $R(F) = \Sigma||F_o| - |F_c||/\Sigma|F_o|$; $R(F^2) = \Sigma w(F_o^2 - F_c^2)^2/\Sigma w(F_o^2)^2$; $S(F^2) = \Sigma w(F_o^2 - F_c^2)^2/(N_D - N_P)$ N_D = no. of data, N_P = no. of parameters.

Table 6 Atomic coordinates ($\times 10^4$) for [Ni(badp)(H_2O)Br]Br and [Cu(badp)(H_2O)]Br_2

	M = Ni			M = Cu		
	x	*y*	*z*	*x*	*y*	*z*
M	7 999(1)	3 125(1)	1 201(1)	7 031(1)	3 351(1)	−1 121(1)
Br(1)	7 793(1)	1 205(1)	2 523(1)	7 227(1)	4 104(1)	2 439(1)
Br(2)	9 156(1)	7 733(1)	396(1)	5 866(1)	8 075(1)	−449(1)
O	8 275(4)	4 487(5)	80(3)	6 755(7)	4 878(8)	95(6)
N(1)	6 303(4)	2 662(4)	396(3)	8 688(6)	2 784(8)	−368(5)
N(2)	6 990(4)	4 539(5)	1 690(3)	8 008(6)	4 587(7)	−1 668(5)
N(3)	8 374(4)	1 436(5)	386(4)	6 585(7)	1 727(8)	−405(6)
N(4)	9 390(4)	4 192(6)	2 264(4)	5 644(7)	4 259(9)	−2 198(6)
C(1)	6 142(5)	1 656(6)	−278(4)	8 818(8)	1 752(8)	296(6)
C(2)	4 959(6)	1 231(6)	−771(4)	9 982(8)	1 267(10)	778(6)
C(3)	3 984(6)	1 866(7)	−558(4)	10 976(9)	1 807(10)	573(7)
C(4)	4 182(5)	2 920(6)	137(4)	10 823(8)	2 875(11)	−129(7)
C(5)	5 355(5)	3 305(5)	609(4)	9 609(7)	3 347(9)	−604(5)
C(6)	5 767(6)	4 418(6)	1 376(4)	9 249(8)	4 417(10)	−1 357(6)
C(7)	5 011(6)	5 278(6)	1 732(4)	9 969(8)	5 249(10)	−1 749(7)
C(8)	5 573(6)	6 298(7)	2 418(4)	9 382(10)	6 529(11)	−2 439(7)
C(9)	6 839(6)	6 417(6)	2 723(4)	8 143(9)	6 396(10)	−2 756(6)
C(10)	7 527(6)	5 494(6)	2 352(4)	7 439(8)	5 501(10)	−2 340(7)
C(11)	7 315(5)	1 102(6)	−447(4)	7 644(9)	1 294(10)	455(6)
C(12)	8 907(6)	5 467(7)	2 632(5)	6 087(9)	5 496(11)	−2 605(7)

Table 7 Selected bond lengths (Å) and angles (°) for the metal co-ordination sphere, with estimated standard deviations in parentheses

(*a*) [Ni(badp)(H_2O)Br]Br

Br(1)–Ni	2.6748(12)	Ni–N(1)	2.001(4)
Ni–N(2)	2.008(5)	Ni–N(3)	2.086(5)
Ni–N(4)	2.119(5)	Ni–O	2.145(4)
N(1)–Ni–N(2)	78.0(2)	N(1)–Ni–N(3)	80.0(2)
N(2)–Ni–N(3)	158.0(2)	N(1)–Ni–N(4)	157.6(2)
N(2)–Ni–N(4)	79.7(2)	N(3)–Ni–N(4)	122.3(2)
N(1)–Ni–O	91.0(2)	N(2)–Ni–O	94.7(2)
N(3)–Ni–O	86.6(2)	N(4)–Ni–O	91.0(2)
N(1)–Ni–Br(1)	89.96(12)	N(2)–Ni–Br(1)	91.73(13)
N(3)–Ni–Br(1)	87.30(14)	N(4)–Ni–Br(1)	90.5(2)
O–Ni–Br(1)	173.57(13)	C(5)–N(1)–Ni	118.5(3)
C(1)–N(1)–Ni	119.3(4)	C(10)–N(2)–Ni	120.3(4)
C(6)–N(2)–Ni	117.9(4)	C(11)–N(3)–Ni	111.5(3)
C(12)–N(4)–Ni	111.3(4)		

(*b*) [Cu(badp)(H_2O)]Br_2

Cu–N(2)	1.957(7)	Cu–N(1)	1.957(7)
Cu–N(3)	2.017(7)	Cu–N(4)	2.044(8)
Cu–O	2.374(7)		
N(2)–Cu–N(1)	78.9(3)	N(2)–Cu–N(3)	160.0(3)
N(1)–Cu–N(3)	82.1(3)	N(2)–Cu–N(4)	81.3(3)
N(1)–Cu–N(3)	159.6(3)	N(3)–Cu–N(4)	116.9(3)
N(2)–Cu–O	98.4(3)	N(1)–Cu–O	95.3(3)
N(3)–Cu–O	89.3(3)	N(4)–Cu–O	92.5(3)
C(1)–N(1)–Cu	118.1(6)	C(5)–N(1)–Cu	117.8(6)
C(10)–N(2)–Cu	118.7(6)	C(6)–N(2)–Cu	117.9(5)
C(11)–N(3)–Cu	111.3(5)	C(12)–N(2)–Cu	110.9(6)

and the two amine nitrogens [116.9° for N(3)–Cu–N(4)] is much larger than that between the metal ion and the two pyridyl nitrogens [78.9° for N(1)–Cu–N(2)], while the four nitrogen donors of the chelating ligand and the central copper ion are almost in the same plane. In the axial direction the Cu–O vector is nearly perpendicular to the basal plane, the four apical N–Cu–O bond angles having a mean value of 93.9°.

Compound **2** crystallizes in the space group $P2_1/c$. The geometry about the six-co-ordinated nickel(II) is best described as distorted octahedral with an oxygen atom of water and one Br^- ion occupying the axial sites, and the two aromatic nitrogen atoms and two amino nitrogens of the badp ligand occupying the four equatorial sites to form the Ni–N_4 equatorial plane, as shown in Fig. 5.

The conformation adopted by badp is quite different from that in the compound [Ni(trien)$(NCS)_2$][15], in which the four nitrogen atoms of trien occupy two apical and two equatorial positions of an octahedron, leaving two *cis* positions for the thiocyanate groups which are bonded *via* their nitrogen atoms. Since the single bonds in the quadridentate trien can freely rotate to co-ordinate the central nickel ion, the sp^3 electron pairs of the N atoms of this ligand do not favour co-ordination of Ni^{II} in the same plane. The intrachelate N–Ni–N bond angles in different planes, which are equal to the mean value of 81.7° within 0.7° of the standard deviation, indicate that the ligand molecule fits the nickel ion adequately to form a stable complex.

In contrast to the nickel(II) complex of trien, the aromatic conjugation effect of bipyridine in the tetradentate badp hinders free rotation, the trigonal sp^2 electron pairs of the aromatic nitrogen donors co-ordinating to the nickel(II) ion in a nearly planar configuration formed by the four nitrogen donor atoms of the ligand. The angles between the metal centre and adjacent donor nitrogens inside the plane are forced to diverge from the ideal value of 90°. For example, N(1)–Ni–N(2), N(1)–Ni–N(3) and N(2)–Ni–N(4) are 78.0(2), 80.0(2) and 79.7(2)°, respectively. Since these angles are so small, N(3)–Ni–N(4) is very large, 122.3(2)°.

Although there are considerable angular irregularities, both metal complexes form nearly planar geometries around their equatorial positions. The mean deviations from the least-squares planes formed by the four nitrogens are only 0.005 Å for the nickel complex and only 0.006 Å for the copper complex. The nickel(II) ion protrudes only 0.013 Å above the plane, toward the co-ordinated water molecule, while the copper(II) ion resides 0.116 Å above the plane and is also directed toward the co-ordinated water molecule.

The crystal structure of badp and those of its complexes **1** and **2** show that the energy of complex formation drives the ligand to adopt a geometry in which the bond between the pyridine rings rotates 180° so that all four nitrogen atoms are on the same side of the bipyridyl ring and in the same plane. However, the co-ordination along the axial direction is much different for the two complexes. As shown in Fig. 5, the six-co-ordinated nickel(II) ion of complex **2** is a distorted octahedron; however, the five-co-ordinated copper(II) ion of complex **1** is a distorted square pyramid. For the copper(II) ion with the d^9 electronic state the elongation of one axis in the presence of ligand-field

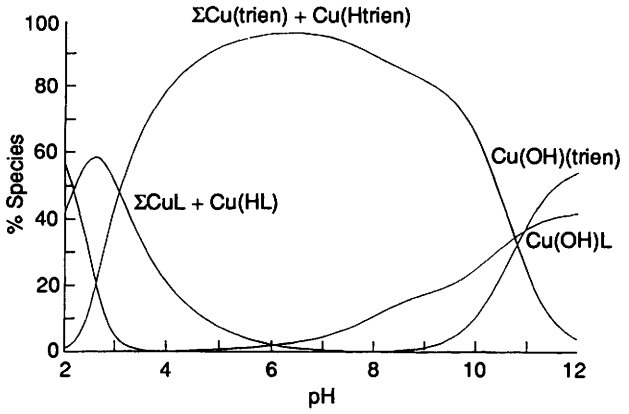

Fig. 6 Distribution of complex species as a function of pH for a system containing a 1 : 1 : 1 ratio of Cu^{II}, badp, and trien at 25.0 °C and 0.100 mol dm^{-3} ionic strength (KCl). Curves show complex formed relative to total concentration of copper(II) species present at 100%

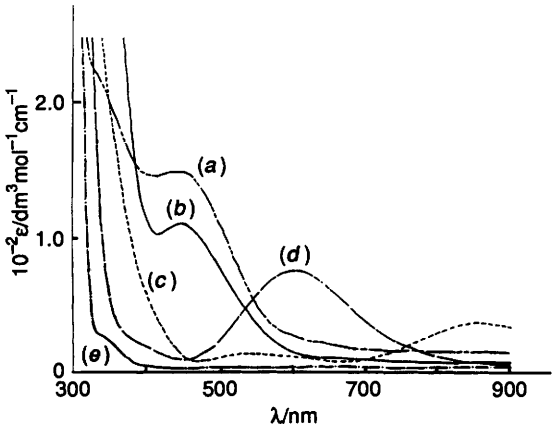

Fig. 7 Electronic spectra of solutions (4.00×10^{-3} mol dm^{-3}) of (*a*) $[Fe(badp)]^{2+}$ (pH 6.9), (*b*) $[Co(badp)]^{2+}$ (pH 6.4), (*c*) $[Ni(badp)]^{2+}$ (pH 6.6), (*d*) $[Cu(badp)]^{2+}$ (pH 6.2) and (*e*) $[Zn(badp)]^{2+}$ (pH 7.1)

stabilization energy distorts the geometry, thus removing the degeneracy of the d orbitals (the Jahn–Teller effect).

It should be pointed out that the stability constants listed in Table 2 for badp are exceptionally low for a tetradentate polyamine. The stability constant of the copper(II) chelate is over five orders of magnitude lower than that with the aliphatic polyamine triethylenetetramine (trien, $10^{20.1}$ dm^3 mol^{-1}). In fact, this stability constant is even lower than that with the analogous tridentate ligand 2,6-bis(aminomethyl)pyridine (bap, $10^{15.7}$ dm^3 mol^{-1}). While the lower stability constant with respect to that of trien can be considered due to the lower basicity of the ligand, it can be only partly so, since the basicity of the analogous ligand *N,N'*-bis(2-pyridylmethyl)ethylenediamine (bpmen) is lower than that of badp, but the stability constants of its chelates with Cu^{II} and Ni^{II} are considerably higher. The influence of ligand basicity on the formation of complexes in solution is seen from the species distribution curves in Fig. 6. It is seen that the Cu(badp) predominates at low pH even though its stability constant is lower, because it is less basic and does not compete as effectively as trien for hydrogen ion. At higher pH where hydrogen-ion competition is less important, the more stable copper(II) complex of trien is seen to predominate even as the hydroxo species.

The exceptionally low stability of the Cu(badp) chelate, which is below that which would have been predicted on the basis of ligand basicity, cannot be due to the differences in ligand preorganization, since both free badp and trien are poorly preorganized for metal complexation. The polar primary amino groups are far apart, in extended positions in solution. However the crystal structure of the copper(II) chelate in Fig. 5 offers a clue. It is seen that the donor nitrogen atoms of the ligand are roughly in the same plane, but that the three angles that the central metal ion makes with the four nitrogens of the ligand are exceptionally small (≈80°), and the angle between the terminal amino groups is especially large (≈120°) so that the co-ordination sphere is somewhat strained relative to a structure in which the donor nitrogens are farther apart and equally spaced. The same observations also apply to the nickel(II) complex (Fig. 5). This additional strain probably applies also to the complexes in solution and could account for the further reduction of the stabilities of the complexes.

These arguments are supported by the comparison of the relative stability constant decreases in going from ethylenediamine to either bipyridyl or to 2-(aminomethyl)pyridine. In the first case for copper(II) this decrease is 1.5 log units and for nickel(II) it is only 0.3 log units. However in comparing the decrease in stability in going from ethylenediamine to 2-(aminomethyl)pyridine the decrease is only 1.0 log units for copper(II) and 0.20 for nickel(II). If the view is taken that in themselves the partial contributions from the individual structural units are only minor then the angular distortions found in the crystal structures must account for the remaining drop in stability constants.

Experimental

Methods and Materials.—All ^1H and ^{13}C NMR spectra were measured with a Varian XL200 FT spectrometer. Chemical shifts are reported relative to tetramethylsilane as an internal standard. Mass spectra were obtained by fast atom bombardment with a VG analytical 70S high-resolution double-focusing magnetic sector spectrometer, with nitrobenzyl alcohol as the matrix solvent, at Mass Spectrometry Applications Laboratory, Texas A & M University. Ultraviolet–visible spectra were recorded on a Perkin-Elmer 553 spectrophotometer. Melting points were determined on a Fisher-Johns apparatus. Elemental analyses were measured by Galbraith Laboratories, Inc., Knoxville, TN. The starting material 2-amino-6-methylpyridine was obtained from Aldrich Chemical Co. and used without further purification. Solvents were appropriately purified, dried and degassed prior to use.

Potentiometric Determinations.—Potentiometric pH measurements and computation of the protonation constants and stability constants were carried out by procedures described in detail elsewhere.[9] The pH measurements were made at 25.0 ± 0.1 °C and ionic strength 0.100 mol dm^{-3} adjusted with KCl. Typical concentrations of experimental solutions were 2.00×10^{-3} mol dm^{-3} in badp and 0.100 mol dm^{-3} in KOH. Typical initial solution volumes were 50.0 cm^3. Forty experimental data points were recorded in the titration of badp; the three parallel titrations were replicated for determination of the standard deviation. Typically, fifty data points were recorded in the titration of each metal ion–badp system. Oxygen and carbon dioxide were excluded from the reaction mixture by maintaining a slight positive pressure of purified argon gas in the reaction cell. Standard stock solutions were prepared from analytical grade $NiCl_2$, $Co(NO_3)_2$, $Cu(NO_3)_2$ and $ZnCl_2$; $FeCl_2$ was prepared from 99.9% iron chips by direct reaction with concentrated hydrochloric acid and then crystallized under nitrogen gas to form a light green crystalline product. The standard stock solution of Fe^{II} was prepared in the presence of added 0.0100 mol dm^{-3} hydrochloric acid. The concentrations of all the above standard stock solutions were analysed quantitatively by cation-exchange measurement (Dowex 50Wx8 resin, 20–50 mesh, hydrogen form). The pH meter–glass electrode system was calibrated by standard acid with KCl as the supporting electrolyte at 0.100 mol dm^{-3} to read hydrogen-ion concentration directly so that the measured quantity was −log

$[H^+]$. The value of log K_w defined as log $([H^+][OH^-])$, was found to be -13.78 at the ionic strength employed.[9] Computations were all carried out with the program BEST[9] and species distributions were calculated with the program SPE[9] and plotted with a Laser Jet II with SPEPLOT.[9]

Synthesis of 6,6'-Bis(aminomethyl)-2,2'-bipyridyl (*see Scheme* 1).—The final product was fully characterized and subjected to elemental analysis. The intermediates were identified by NMR spectroscopy.

2-Bromo-6-methylpyridine. 2-Amino-6-methylpyridine (108 g, 1 mol) was dissolved in 48% HBr (350 cm^3) in a three-neck flask (2 l) which was cooled by an ice–salt bath and stirred mechanically. Bromine (100 cm^3, 2 mol) was added dropwise and a yellow solid formed. Then, a saturated aqueous solution of sodium nitrite (138 g, 2 mol in 210 cm^3 water) was added slowly and a brown gas was evolved. The reaction mixture was brought to pH > 11 with sodium hydroxide, extracted with dichloromethane, dried over magnesium sulfate, and the organic solvent evaporated to produce an oil, which was distilled: b.p. 48.5–49.5 °C (3 mmHg) [lit.,[6] b.p. 62–65 °C (4 mmHg)], 148 g (86%); ^{1}H NMR ($CDCl_3$): δ 2.54 (s, CH_3, 3 H), 7.11 (d, H^5, J = 7.5, 1 H), 7.29 (d, H^3, J = 7.5, 1 H), and 7.43 (t, H^4, J = 7.5 Hz, 1 H).

6,6'-Dimethyl-2,2'-bipyridyl. A mixture of 2-bromo-6-methylpyridine (138 g, 0.8 mol), sodium formate (68 g, 1 mol), 10% wet Pd/C (5 g), benzyltriethylammonium chloride monohydrate (25 g, 0.1 mol), 10 mol dm^{-3} NaOH (70 cm^3), and water (200 cm^3) was refluxed for 7 d. Additional sodium formate (3 g) and 10% wet Pd/C catalyst (0.3 g) were added each day. The mixture was finally filtered, extracted with dichloromethane, dried over magnesium sulfate and evaporated to give a crude oil which crystallized to a white crystalline product after standing for 24 h at room temperature. The crude oil was distilled in *vacuo* to give the desired product: b.p. 108–109 °C (5 mmHg), 49.7 g (67%), m.p. 90.5–91.5 °C (lit.,[6] m.p. 88–89 °C); ^{1}H NMR ($CDCl_3$): δ 2.62 (s, CH_3, 6 H), 7.14 (d, $H^{5,5'}$, J = 7.4, 2 H), 7.68 (t, $H^{4,4'}$, J = 7.4, 2 H), and 8.18 (d, $H^{3,3'}$, J = 7.4 Hz, 2 H).

6,6'-Bis(bromomethyl)-2,2'-bipyridyl. A reaction mixture of 6,6'-dimethyl-2,2'-bipyridyl (22.1 g, 0.120 mol), *N*-bromosuccinimide (42.6 g, 0.240 mol), benzoyl peroxide (250 mg) as catalyst and CCl_4 (1200 cm^3) was refluxed for 1 h; then more imide (2.1 g, 0.012 mol) and catalyst (200 mg) were added. The mixture was refluxed for 5 h, cooled to 35 °C and the succinimide filtered off. The filtrate was evaporated to 120 cm^3 and cooled to 4 °C for 12 h. The solid which deposited was filtered off and recrystallized from chloroform (160 cm^3) to give the required product (14.5 g, 35%) as a white crystalline solid. Both the CCl_4 and $CHCl_3$ filtrates obtained above were evaporated to remove the solvent. The residue was separated by flash chromatography on a silica column with CH_2Cl_2–$CHCl_3$ (9:1) to give another crop (8.6 g, 21%), 6-bromomethyl-6'-methyl-2,2-bipyridine (3.3 g, 8%), and 6,6'-bis(dibromomethyl)-2,2'-bipyridine (6.2 g, 15%). Total yield of required product: 23.1 g (*ca.* 56%). ^{1}H NMR ($CDCl_3$): δ 4.63 (s, CH_2, 4 H), 7.46 (d, $H^{5,5'}$, J = 7.8, 2 H), 7.83 (t, $H^{4,4'}$, J = 7.8, 2 H), and 8.38 (d, $H^{3,3'}$, J = 7.8 Hz, 2 H).

6,6'-Bis(aminomethyl)-2,2'-bipyridyl trihydrobromide salt. A solution of 6,6'-bis(bromomethyl)-2,2'-bipyridyl (8.5 g, 25 mmol) in $CHCl_3$ (320 cm^3) was refluxed and dissolved completely; then hexamethylenetetraamine $[(CH_2)_6N_4]$ (7.6 g, 54 mmol) in $CHCl_3$ (200 cm^3) was added dropwise. A white precipitate formed and the mixture was refluxed for 4 h. The mixture was allowed to cool to room temperature and to stand for 24 h. The solid deposit was filtered off, dried *in vacuo*, and suspended in water (70 cm^3)–EtOH (300 cm^3)–48% HBr (50 cm^3). The mixture was stirred at 75 °C until the solid had completely dissolved. The solution was allowed to stand for 24 h at room temperature and the crystalline needles of badp·3HBr·H_2O formed were filtered off and dried: 8.4 g (71%). ^{1} NMR (D_2O): ^{1}H, δ 4.62 (s, CH_2, 4 H), 7.80 (d, $H^{5,5'}$, J = 7.6, 2 H), 8.31 (t, $H^{4,4'}$, J = 7.7, 2 H), and 8.52 (d, $H^{3,3'}$, J = 7.6 Hz, 2 H); ^{13}C, δ 40.8 (CH_2NH_2); 122.2, 124.5, 141.7, 148.6 and 149.6 (CH of bipy) (Found: C, 30.55; H, 4.30; Br, 49.80; N, 11.75. Calc. for $C_{12}H_{14}N_4$·3HBr·H_2O: C, 30.35; H, 4.05; Br, 50.45; N, 11.80%). Mass spectrum: *m/z* 215 ($[M + H]^+$).

Crystalline badp·2HCl·H_2O. A sample of badp·3HBr (95 mg, 0.20 mmol) was dissolved in water (4.0 cm^3). Then 0.100 mol dm^{-3} standard KOH solution was added slowly until the pH was 5.0. Then KCl (370 mg) was added as a matrix. The clear solution was allowed to evaporate to the atmosphere through a small opening. Colourless crystals which formed over a period of 6–8 d were found to be suitable for structure determination.

Crystalline [Cu(badp)(H_2O)]Br_2, **1**.—A sample (48 mg, 0.10 mmol) of badp·3HBr·H_2O and $CuCl_2$·$2H_2O$ (17 mg, 0.10 mmol) were dissolved in distilled water (5 cm^3). Then 0.100 mol dm^{-3}, KOH solution was added slowly until the pH reached 4.1. The solution was heated to 55 °C to reduce the volume of the filtrate by ≈25% and then allowed to evaporate to the atmosphere at room temperature to afford the product as dark blue crystals.

Crystalline [Ni(badp)(H_2O)Br]Br_2, **2**.—A sample of badp·3HBr·H_2O (0.10 mmol; 0.0101 mol dm^{-3}, 10.0 cm^3) was treated with $NiCl_2$ (0.10 mmol; 0.0100 mol dm^{-3}, 10.0 cm^3). The mixture was adjusted to pH 7.1 by addition of 0.100 mol dm^{-3} KOH. The colour gradually changed from light blue to green. Evaporation at 60 °C to reduce the volume by one tenth was followed by slow cooling to room temperature. This procedure afforded dark green crystals suitable for X-ray diffraction study.

Structure Determinations.—A colourless plate (0.21 × 0.22 × 0.32 mm) of badp·2HCl·H_2O, a dark green parallepiped (0.15 × 0.21 × 0.33 mm) of complex **1**, and a dark blue needle (0.21 × 0.33 × 0.11 mm) of **2** were mounted on glass fibres with epoxy cement at room temperature. Preliminary examination and data collection were performed on a Rigaku AFC5R diffractometer for badp and **2** and a Siemens R3m for **1**. Cell parameters were calculated from the least-squares fitting of the setting angles for 25 reflections.

Data were collected for $4.0 \leqslant 2\theta \leqslant 50.0°$ for badp, **1** and 4.0–120° for **2** at 293 K. The weak reflections were rescanned (maximum of two rescans) for badp and **2** and the counts for each scan were accumulated. Three control reflections, collected every 150 for badp and **2**, and every 97 for **1**, showed no significant trends. Background measurement was made by the stationary crystal and stationary counter technique at the beginning and end of each scan for half of the total scan time.

Lorentz and polarization corrections were applied to 1403, 2617 and 2320 reflections for badp, **1** and **2**, respectively. A semiempirical absorption correction was applied for all three structures. The structures were solved by direct methods.[16] Full-matrix least-squares anisotropic refinements[17] were carried out for all non-hydrogen atoms. Hydrogen atoms were placed in idealized positions with isotropic thermal parameters fixed at 0.08 $Å^2$. Neutral atom scattering factors and anomalous scattering correction terms were taken from ref. 18.

Additional material available from the Cambridge Crystallographic Data Centre comprises H-atom coordinates, thermal parameters and remaining bond lengths and angles.

Acknowledgements

This work was supported by a grant, A-259, from The Robert A. Welch Foundation. The R3m/V single-crystal X-ray diffraction and crystallographic computing system in the Crystal and Molecular Structure Laboratory of the Department of Chemistry, Texas A & M University, was purchased with funds provided by the National Science Foundation.

References

1 B. Alpha, E. Anklam, R. Deschenaux, J. M. Lehn and M. R. Pietraskiewicz, *Helv. Chim. Acta*, 1988, **71**, 1042.
2 F. Barigelletti, L. De Cola, V. Balzani, P. Belser, A. von Zelewsky, F. Vögtle, F. Ebmeyer and S. Grammeenudi, *J. Am. Chem. Soc.*, 1989, **111**, 4662.
3 K. E. Krakowiak, J. S. Bradshaw, W. Jiang, N. K. Dalley, G. Wu and R. M. Izatt, *J. Org. Chem.*, 1991, **56**, 2675.
4 R. Ziessel, M. Maestri, L. Prodi, V. Balzani and A. V. Dorsselaer, *Inorg. Chem.*, 1990, **32**, 1237.
5 F. Ebmeyer and F. Vögtle, *Chem. Ber.*, 1989, **122**, 1725.
6 G. R. Newkome, D. C. Pantaleo, W. E. Puckett, P. L. Ziefle and W. A. Deutsch, *J. Inorg. Nucl. Chem.*, 1981, **43**, 1529.
7 J. C. Rodriguez-Ubis, B. Alpha, D. Plancherel and J. M. Lehn, *Helv. Chim. Acta*, 1984, **67**, 2264.
8 J. de Mendoza, E. Mesa, J. C. Rodriguez-Ubis, P. Vazgues, F. Vögtle, P. M. Windscheif, K. Rissanen, J. M. Lehn, D. Lilienbaum and R. Ziessel, *Angew. Chem., Int. Ed. Engl.*, 1991, **30**, 1331.
9 A. E. Martell and R. J. Motekaitis, *Determination and Use of Stability Constants*, 2nd edn, VCH, New York, 1992.
10 Y. Couturier and C. Petitfaux, *Bull. Soc. Chim. Fr.*, 1975, 1545.
11 R. M. Smith and A. E. Martell, *Critical Stability Constants*, Plenum, New York, 1989, vol. 6.
12 R. G. Lacoste and A. E. Martell, *Inorg. Chem.*, 1964, **3**, 881.
13 C. K. Johnson, ORTEP, Report ORNI-5138, Oak Ridge National Laboratory, Oak Ridge, TN, 1976.
14 G. Marongiu, E. C. Lingafelter and P. Paoletti, *Inorg. Chem.*, 1969, **8**, 2763.
15 A. Clausen and A. Hazell, *Acta Chem. Scand.*, 1970, **8**, 2811.
16 G. M. Sheldrick, SHELXS 86, Program for Crystal Structure Solution, University of Göttingen, 1986.
17 G. M. Sheldrick, SHELXS 93, Program for Crystal Structure Refinement, Göttingen, 1993.
18 *International Tables for X-Ray Crystallography*, ed. T. Hahn, D. Reidel, Dordrecht, distributed by Kluwer Academic Publishers, 1992.

Received 26*th September* 1994; *Paper* 4/05821F